Journal of Hydrology 504 (2013) 94–103

Contents lists available at ScienceDirect

Journal of Hydrology

journal homepage: www.elsevier.com/locate/jhydrol

Variation of soil infiltrability across a 79-year chronosequence of naturally restored grassland on the Loess Plateau, China

Yonggang Zhao [a,b,c], Pute Wu [a,b,c], Shiwei Zhao [b,*], Hao Feng [a,b,c]

[a] College of Water Resources and Architectural Engineering, Northwest A&F University, Yangling 712100, Shaanxi, China
[b] Institute of Soil and Water Conservation, Northwest A&F University, Yangling 712100, Shaanxi, China
[c] Institute of Water Saving Agriculture in Arid Regions of China, Northwest A&F University, Yangling 712100, Shaanxi, China

ARTICLE INFO

Article history:
Received 17 July 2013
Received in revised form 22 September 2013
Accepted 23 September 2013
Available online 1 October 2013
This manuscript was handled by Geoff Syme, Editor-in-Chief

Keywords:
Soil infiltration
Rainfall simulation
Semi-arid hydrology
Runoff plot
Soil structure
Soil organic matter

SUMMARY

Soil infiltrability plays a critical role in controlling soil erosion and enhancing water storage in arid and semi-arid areas. Presently, knowledge is lacking regarding the dynamic mechanism and characteristics of soil infiltration during long-term natural vegetation restoration. This study evaluated how soil infiltrability changes along a 79-year chronosequence of natural restoration from cropland to permanently restored grassland. A slope cropland (control) and five grasslands of successive age-classes (6-, 16-, 36-, 56-, and 79-year natural restoration treatments) were selected to establish a chronosequence on China's Loess Plateau. Soil infiltrability was measured under simulated rainfall conditions at three intensities (20, 40, and 60 mm/h) using a run off–on–out method. The steady-state infiltration rate (SIR) of the control treatment decreased with increasing intensity of rainfall while those of the natural restoration treatments showed a contrary tendency. With the extension of restoration period, the SIR was gradually increased while the runoff was decreased and the time-to-runoff and time-to-SIR were prolonged. The SIR had a significant negative exponential relationship with the restoration period under different rainfall conditions ($P < 0.01$). Soil infiltrability showed rapid increases within 16 year of natural restoration and slight changes thereafter. Soil parameters including SIR and the contents of macroaggregates (>0.25 mm) and organic matter were significantly correlated with each other ($P < 0.01$). Long-term natural restoration of grassland, especially for 16-year, significantly enhanced soil infiltrability and reduced soil erosion through organic matter accumulation and the resulting improvement of structural properties. This study provides reference data for describing hydrological parameters on the Loess Plateau.

1. Introduction

Rainfall infiltration is an important process of the water cycle in terrestrial ecosystems. Being an important hydrologic parameter, the infiltration rate (IR) determines soil water storage and runoff. In arid and semiarid regions, soil function is sensitive to structural degradation and highly variable precipitation which potentially threaten the eco-environment and agricultural production (Ben-Hur and Lado, 2008; Chartier et al., 2011). For example, on the Loess Plateau in China, soil structure is unstable and strong rainfall (mainly concentrated in June–September) leads to serious loss of soil and water (Shi and Shao, 2000). Associated hydro-geochemical processes may promote the silt up of rivers and potentially threaten the safety of the Yellow River Basin (Shi and Shao, 2000; Tang et al., 1998).

A key strategy for reducing runoff and soil erosion hazards is to retain and infiltrate more precipitation locally (Zhu, 2006). In many arid and semiarid regions of the world, natural or artificial vegetation restoration by converting slope cropland to forest or grassland has widely been used for restoring degraded ecosystems. Artificial vegetation restoration is expected to accelerate the positive succession of vegetation and shorten the time required for approaching a stable stage (Jiao et al., 2007). However, the restoration activity is commonly associated with negative ecological impacts such as plant growth restriction, dried soil layer formation (Wang et al., 2010), and soil quality degradation. In view of these issues, better understanding of the dynamic mechanism and characteristics of infiltration during natural vegetation restoration is considered important for providing reference of sustainable eco-environmental construction on the Loess Plateau. Presently, research is lacking on the changes in soil infiltrability across a restoration chronosequence of natural grassland.

The infiltration capacity of soil is mainly controlled by rainfall intensity and soil properties (Abu-Hamdeh et al., 2006; Assouline,

* Corresponding author. Tel.: +86 29 87011863.
E-mail address: swzhao@ms.iswc.ac.cn (S. Zhao).

0022-1694/$ - see front matter © 2013 Elsevier B.V. All rights reserved.
http://dx.doi.org/10.1016/j.jhydrol.2013.09.039

2004; Franzluebbers, 2002). Higher rainfall intensity means higher raindrop kinetic energy that can more rapidly wet the soil surface and significantly impact the soil structure, leading to physical disintegration of soil aggregates (Agassi et al., 1985). These processes contribute to the formation of a structural seal on soil surface that can reduce the infiltration capacity of soil (Agassi et al., 1981). In addition, surface soil structural properties, such as soil organic matter (SOM) content, bulk density (BD), aggregate size distribution, and aggregate stability, impose strong influences on the IR (Abu-Hamdeh et al., 2006; Franzluebbers, 2002; Lado et al., 2004a). For example, the steady-state IR (SIR) rises with increasing SOM content, aggregate size, and aggregate stability in a sandy loam (Humic Dystrudept) (Lado et al., 2004a, 2004b). However, previous studies on the relationship between soil infiltrability and structural properties are mostly based on laboratory experiment with sieved-soil. Quantitative information is lacking on soil infiltrability as influenced by the structural properties under field conditions.

The effects of vegetation restoration on soil properties have been studied extensively. During vegetation restoration, soil properties generally undergo dynamic changes over time due to plant-induced effects (Angers and Caron, 1998; Li and Shao, 2006). It has been found that on the Loess Plateau, there are decreases in soil BD and increases in the contents of SOM and macroaggregates (>0.25 mm) as well as the aggregate stability across a chronosequence of naturally restored vegetation (An et al., 2009; Jiao et al., 2011; Li and Shao, 2006). The increase in SOM content and improvement of soil structural properties can jointly influence soil infiltration characteristics (Abu-Hamdeh et al., 2006; Bo et al., 2007; Elliott and Efetha, 1999). Despite the known effects of vegetation restoration on soil properties and the IR, the response of soil infiltrability to the succession of natural grassland vegetation under rainfall conditions remains unclear. Especially, the changes in soil's infiltration capacity related to soil development during natural vegetation restoration are not fully understood.

In view of the close relationship between soil structural properties and infiltration, we hypothesized that soil structure changed across a chronosequence of naturally generating vegetation and thus affected the infiltration capacity of soil under rainfall conditions. The objectives of the present study were: (1) to evaluate the infiltration capability of soil as influence by restoration of natural grassland vegetation under simulated rainfall conditions; and (2) to describe the changes in soil structural properties during natural grassland vegetation restoration and analyze the relationship between soil properties and infiltration. The results will provide new insights into the effect of natural vegetation restoration on infiltration and further provide baseline reference for rational vegetation restoration and soil–water conservation on the Loess Plateau and other similar settings.

2. Materials and methods

2.1. Study area description

This study was conducted in a grassland in the Yunwu Mountain Natural Reserve (36°13′–36°19′N, 106°24′–106°28′E), Guyuan City, Ningxia Hui Autonomous Region, China. The natural reserve (including core, buffer, and experimental areas) was established in 1982 on western Loess Plateau (Fig. 1). Presently, *Stipa bungeana* is the only remaining species of typical grassland in the reserve area. The natural reserve (1800–2148 m above sea level) covers an area of 7000 hm^2, with approximately 90% grass hill and only 6% slope cropland for intensive agriculture. The natural reserve has a moderate (temperate) semi-arid climate. The evaporation is 1330–1640 mm, with a mean aridity index of 1.8 and an annual mean air temperature of 5 °C. Sixty-year mean annual precipitation is 412 mm per year, of which more than 65% falls during July–September. Mean annual frost-free period is 137 d (Zou et al., 1997; An et al., 2009). The major soil types are loessial soil and Heilu soil, and the majority of slope cropland soil is loessial soil. The soil profile is relatively uniform in terms of texture and structure. Groundwater level is significantly low with nearly no recharge to the soil surface layer.

2.2. Experimental design and soil sampling

Based on field survey and previous researches of plant succession in the study area (Zou et al., 1997), a chronosequence of natural vegetation succession series was established by selecting abandoned slope croplands with naturally restored grassland vegetation of different age-classes, i.e., 6-, 16-, 36-, 56-, and 79-year. A slope cropland was used as control. The basic soil properties and vegetation characteristics of the selected slope cropland and naturally restored grasslands are summarized in Table 1. For each treatment, three study plots (6 m × 6 m) were randomly located and considered as replicates. The plots were chosen at the lower slope, at least 15 m apart from each other and 15 m away from the boundary of the experimental site.

2.3. Rainfall simulation

Rainfall infiltration measurements were conducted with a rainfall simulator in July 2006. Soil infiltrability was determined using a run off–on–out method (Lei et al., 2006; Liu et al., 2011). Rainfall simulation experiment was carried out using a movable rain simulator of dripper type (Fig. 2) to give more precise and uniform rainfall intensity than a sprinkler rainfall simulator system. This simulator system generated a broad range of rainfall intensity with the repeatability error <5.5% and the uniformity coefficient >0.97. The raindrop diameter provided by the rainfall simulator ranged from 0.20 to 3.65 mm with increasing rainfall intensity. The device consisted of a water feeder, a rain simulator with dripper, and an infiltration-measuring device. An approximately 5-m^3 plastic water bucket was used as water feeder in the field experiment. The rain simulator (2 m × 0.5 m) formed rainfall at the intensity of 20–60 mm/h as controlled by water depth. The infiltration-measuring device divided the underlay soil surface into the runoff and infiltration sections, with three replicate sub-sections (1 m × 0.15 m each) along the slope (Fig. 2). The runoff section was covered with impermeable materials, and all the rainfall at this section formed running off water flow for the water requirement of the infiltration section. The infiltration section was uncovered and received both the rainwater directly above it and the water flow from the runoff section. More detailed information of the rainfall simulator was described elsewhere (Lei et al., 2006). The computational model for IR (Lei et al., 2006) is expressed as follows:

$$i_1 = P\left(\frac{x_1 W}{A} + 1\right) \tag{1}$$

$$i_2 = P\left(1 + \frac{x_1}{x}\right) - \frac{q}{A\cos\alpha} \tag{2}$$

where i_1 is the IR during run-on advancing (mm/h); i_2 is the IR during the run-out period (mm/h); P is the rain intensity (mm/h); W is the width of soil surface (m); X is the slope length of the infiltration section (m); X_1 is the slope length for water runoff (m); t is time (h); A is the advanced area of run-on water (mm^2); α is the slope gradient in degrees; and Q is the cumulative volume of run-out water (m^3).

According to the results of statistical analysis of precipitation and erosion by Jiao et al. (1999), short-duration, high-intensity

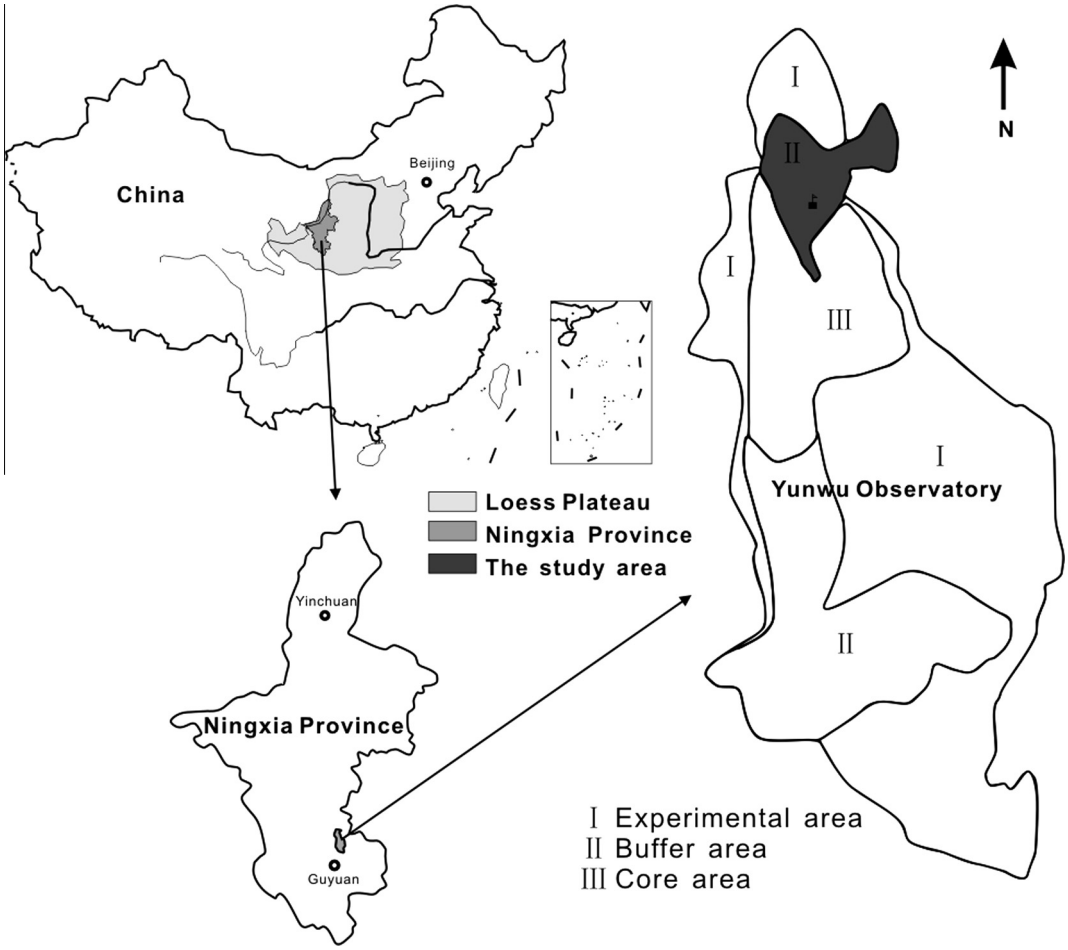

Fig. 1. Location of the study area in the Yunwu Observatory on the Loess Plateau, China.

Table 1
Initial soil properties and vegetation types of slope cropland (SC) and abandoned 6- (NR6), 16- (NR16), 36- (NR36), 56- (NR56), and 79-year-old (NR79) naturally restored grasslands.

Property	SC	NR6	NR16	NR36	NR56	NR79
Sand (>0.02 mm) (%)	22.2	20.4	16.9	13.4	14.3	11.6
Silt (0.02–0.002 mm) (%)	65.2	66.8	69.5	72.7	71.4	74.1
Clay (<0.00 2 mm) (%)	12.6	12.8	13.6	13.9	14.3	14.3
Soil texture (ISSS)	Silt loam	Silt loam	Silt loam	Silt loam	Silt loam	Silt loam
Antecedent soil moisture (%)	9.9	12.5	7.9	8.6	6.9	7.3
Slope (%)	13.3	13.3	20.7	17.3	13.3	18.3
Elevation (m)	2037	2083	2089	2038	2074	2028
Coordinate	106°23′05.4″E, 36°15′42.5″N	106°23′14.1″E, 36°15′47.7″N	106°23′15.9″E, 36°15′55.3″N	106°23′20.4″E, 36°15′06.2″N	106°23′25.9″E, 36°15′42.0″N	106°23′06.7″E, 36°15′19.4″N
Aspect	Semi-sunny	Semi-sunny	Sunny	Semi-shady	Sunny	Semi-shady
Vegetation dominant species	*Avena sativa*	*Leymus secalinus*	*Artemisia sacrorum*	*Artemisia sacrorum*	*Stipa bungeana*	*Stipa grandis*
Auxiliary species		*Heteropappus alataicus*, *Artemisia scoparia*	*Stipa bungeana*, *Anaphalis sinica*	*Thymus mongolicus*, *Stipa bungeana*	*Artemisia sacrorum*, *Heteropappus alataicus*	*Stipa bungeana*, *Artemisia sacrorum*

rainstorm defined as Pattern A storm is the major type of storms that causes severe soil and water loss on the Loess Plateau. The Pattern A storm generally lasts less than 60 min, whose maximum rainfall in 60 min ranges from 12.1 to 64.0 mm and accounts for 85–100% of the total rainfall. Thus we selected the gradient rainfall intensities of 20, 40, and 60 mm/h and the rainfall duration of 60 min to analyze the effects of rainfall conditions on soil infiltration.

The computation of IR involved two stages: In the run-on stage, the IR was computed with model (1) according to the advancing area of runoff water on the infiltration section that was recorded with a digital camera at designated time intervals and quantified from the digital images (Fig. 3) using AutoCAD (Autodesk Inc., USA); In the run-off stage, the IR was computed with model (2) according to the volume of run-out water measured with a glass cylinder when the runoff excessed the infiltration section.

Fig. 2. Photograph of the run off–on–out rainfall simulator used for infiltration test.

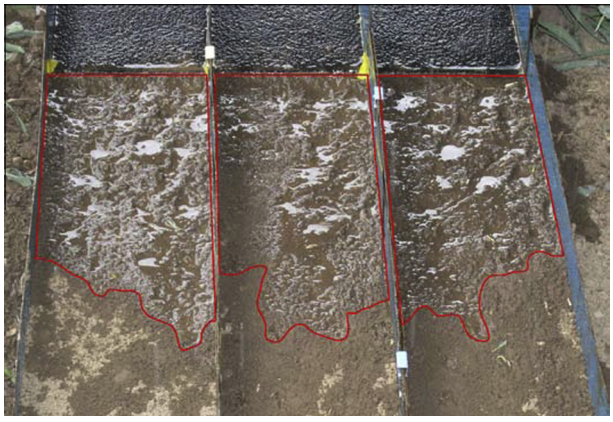

Fig. 3. The advancing area of runoff water on the infiltration section quantified from digital images using AutoCAD.

Before rainfall simulation, the aboveground vegetation on the plots of the infiltration section was cut by shearing. Additionally, the litter layer was removed in order to determine the true infiltration capacity of soil. The device of runoff section was installed at the same gradient with the infiltration section. Both of the runoff and infiltration sections were covered with a plastic film. Then, the rainfall simulator was installed above the two sections, adjusted to the horizontality, and connected with the water feeder. When water level in the simulator met the requirement of specific rainfall intensity, the plastic film cover was removed and the experiment was begun. For more efficient use of water stored in the bucket, we arranged rainfall at decreasing intensity from 60 to 20 mm/h. The rainfall intensity was verified before IR measurement.

2.4. Soil sampling and analyses

Surface soil samples were collected from the 0–10 cm depth in an undisturbed area outside the simulated rainfall experiment area. In each treatment, three plots (20 m × 20 m) were selected with the litter layer removed. In each plot, three samples were randomly collected to form a composite sample, and two soil cores (5 cm × 5 cm) were randomly taken with a stainless cylinder for laboratory assays of soil moisture and BD. A total of 18 composite samples and 36 core samples were obtained and used for laboratory analyses of organic carbon content, particle size distribution, and aggregate stability. The soil samples were sealed in plastic bags and transported to the laboratory. Fresh composite samples were air-dried at room temperature, with large roots and organic residues manually removed. The dry samples were gently crushed and passed through a 2-mm sieve, except for those for aggregate stability analysis. The physicochemical properties of soil samples are presented in Table 1.

Soil particle size distribution was determined using a MasterSizer2000 laser sizer (Malvern Instruments Ltd., Malvern, UK). SOM content was determined using the dichromate oxidation method (Nelson and Sommers, 1982). Soil cores were oven-dried at 105 °C for 24 h to determine the gravimetric water content and compute the BD using a core method (Blake and Hartge, 1986). Soil aggregate stability was measured by using a wet sieving method (Yoder, 1936). Approximately 50 g of air-dried soil samples were placed on a filter paper on a glass dish and moistened by capillarity for 30 min. Then, the soil samples were transferred onto the first sieve of the sequential nest with openings of 5, 2, 1, 0.5, and 0.25 mm diameter. Distilled water was immediately added to the sieve device before the start of the wet sieving process. The samples were then sieved in distilled water at 37 oscillations per minute for 10 min. Soil aggregates retained on each sieve were transferred into clean beakers and oven-dried at 105 °C for 24 h. The dried aggregates from each size class were weighed to calculate the percentage of water-stable aggregates. The aggregate mass of <0.25 mm size was obtained by difference. Three soil samples were replicated with each field sample. The mean weight diameter (MWD) of water-stable aggregates was determined according to the percentage of aggregates of the sizes >5, 2–5, 1–2, 0.5–1, 0.25–0.5, and <0.25 mm (van Bavel, 1950). Large macroaggregates were defined as the >2 mm size fraction; small macroaggregates were defined as the 2–0.25 mm size fraction; and microaggregates were defined as the <0.25 mm size fraction.

Ten sampling cubes (10 cm × 10 cm × 10 cm) were randomly taken in each treatment for root volume determination. The roots were washed to remove soil and then air-dried at room temperature. The root volume was measured using a drainage water method. The total drainage volume from each container (1000-ml cylinder) was collected and measured.

2.5. Statistical analysis

Statistical analysis was performed using the SPSS 18.0 statistical software (SPSS Inc., USA). One-way analysis of variance was used to examine the effects of natural restoration treatments on soil physicochemical properties including SOM (g/kg), BD (g/cm^3), percentage of water-stable aggregates (%), and MWD (mm), and the effects of rainfall intensities (20, 40 60 mm/h) on soil infiltration and runoff including SIR (mm/h) time-to-runoff (min), time-to-SIR (min), and runoff (L). Multiple comparisons of means were accomplished using the method of least significant difference with the significant levels at $P < 0.05$. Correlation analysis between water infiltration and soil properties was conducted using the Origin 8.0 software (OriginLab Corporation, USA).

3. Results

3.1. SOM and BD under natural revegetation

There were significant differences in the SOM content and BD among the natural restoration treatments ($P < 0.01$, Table 2). The SOM content increased significantly with increasing period of

Table 2
Soil organic matter content (SOM) and bulk density (BD) of slope cropland (SC) and abandoned 6- (NR6), 16- (NR16), 36- (NR36), 56- (NR56), and 79-year-old (NR79) naturally restored grasslands.

Treatment	SOM (g/kg)	BD (g/cm^3)
SC	13.4 f	0.97 a
NR6	17.5 e	1.02 a
NR16	20.5 d	0.96 a
NR36	27.3 c	0.95 a
NR56	29.3 b	0.83 b
NR79	31.9 a	0.84 b

Means with different letters in the same column are significantly different at the 0.05 level (LSD).

natural restoration ($P < 0.05$, Table 2). The highest SOM content (31.91 g/kg) was found in the 79-year natural restoration treatment, approximately 2.4-time that of the slope cropland (control). In contrary, the BD showed a decreasing tendency with increasing period of natural restoration. The BD was significantly lower in the 56- and 79-year natural restoration treatments than in the other treatments ($P < 0.05$, Table 2). Soil under 6-year-old natural restoration treatment had slightly higher BD than those of the control and 36-year-old natural restoration treatment, but the difference was not statistically significant ($P > 0.05$).

3.2. Size distribution and stability of water-stable aggregates

Natural restoration of grassland imposed significant effects on the size distribution and stability of water-stable aggregates ($P < 0.01$, Table 3). The proportion of macroaggregates (>0.25 mm) increased significantly with increasing period of vegetation restoration. Water-stable aggregates in the control and 6-year natural restoration treatment were dominated by microaggregates (<0.25 mm) followed by small macroaggregates (2–0.25 mm), and large macroaggregates (>2 mm) made up the smallest proportion. In the 16-year natural restoration treatment, the proportion of large macroaggregates significantly increased from 41.6% to 46.0% ($P < 0.05$), while that of microaggregates significantly decreased from 39.6% to 33.4% ($P < 0.05$). The 79-year natural restoration treatment had the largest proportion of large macroaggregates and the smallest proportion of microaggregates, showing 3.3-time increase and 1.7-time decrease compared to the control, respectively. No significant differences were found in the proportion of large macroaggregates among the 36-, 56-, and 79-year natural restoration treatments ($P > 0.05$).

Additionally, natural restoration had a significant effect on the MWD of water-stable aggregates. The aggregate MWD in the 79-year natural restoration treatment was 2.5-time greater than that of the control treatment, with no significant differences between the 36- and 56-year natural restoration treatments. The variation trend in aggregate MWD is similar to that in macroaggregate (>0.25 mm) content.

3.3. Infiltration under rainfall conditions

The rainfall intensity significantly affected infiltration in the control and natural restoration treatments regardless of the restoration period ($P < 0.01$). The original IR was found relatively high in the infiltration curves of all treatments (Fig. 4). In the control treatment, the IR significantly decreased with increasing intensity of rainfall, and the decreasing rate was lower under low-intensity rainfall (20 mm/h) than under medium- and high-intensity rainfall (40 and 60 mm/h, respectively). The IR under low-intensity rainfall was 1.3- and 1.5-time those under medium- and high-intensity rainfall, respectively. With increasing intensity of rainfall, the time-to-runoff and time-to-SIR decreased while the runoff increased significantly (Table 4).

Similar changes were observed in the soil infiltration curves of natural restoration treatments in an early infiltration stage (approximately 30 min), and higher IRs were detected under lower-intensity rainfall. After 30-min simulated rainfall, the IRs of natural restoration treatments showed substantially different variations from those of the control treatment. Regardless of the restoration history, the IRs of all natural restoration treatments gradually increased with increasing intensity of rainfall, and the corresponding SIRs were significantly higher under high-intensity rainfall than under medium- and low-intensity rainfall ($P < 0.05$). As compared to low-intensity rainfall, high-intensity rainfall increased the SIRs of 6-, 16-, 36-, 56-, and 79-year natural restoration treatments by 19.5%, 38.2%, 20.0%, 19.6%, and 39.3%, respectively. The variation tendencies of the corresponding time-to-runoff, time-to-SIR, and runoff under different rainfall conditions were similar to those of the control treatment, despite that we did not measure the amounts of runoff in the natural restoration treatments under low-intensity rainfall. The infiltration curves of natural restoration treatments under medium- and high-intensity rainfall were similar.

3.4. Infiltration under natural revegetation treatments

Under the same rainfall conditions, the infiltration curves of natural restoration treatments showed great differences (Fig. 5). Higher IRs were observed in the treatment with a longer period of natural restoration. The SIRs showed rapid increases during early-stage natural restoration (<16-year), with slight increases followed by a peak value in the late restoration stage.

The results of non-linear regression analysis showed that there was a negative exponential relationship between SIR and the period of natural restoration under different rainfall conditions ($P < 0.01$, Fig. 6). The simulated curves of the natural restoration treatments were similar under medium- and high-intensity rainfall, especially when the period of natural restoration was greater than 16-year.

Table 3
Percentages of water-stable aggregates of different size-classes and mean weight diameters (MWD) of aggregates at 0–10 cm depth in slope cropland (SC) and abandoned 6- (NR6), 16- (NR16), 36- (NR36), 56- (NR56), and 79-year-old (NR79) naturally restored grasslands.

Treatment	Percentage of water-stable aggregates (%)						MWD (mm)
	>5 mm	5–2 mm	2–1 mm	1–0.25 mm	<0.25 mm	>0.25 mm	
SC	6.9 c	6.9 e	7.6 bc	22.3 ab	56.3 a	43.7 c	0.91 c
NR6	6.5 c	8.9 de	9.3 a	24.3 a	51.0 a	49.0 c	0.99 c
NR16	18.1 b	10.6 cd	8.9 ab	18.8 b	43.5 b	56.5 b	1.58 b
NR36	27.1 a	14.5 ab	5.9 d	12.9 c	39.6 bc	60.4 ab	2.08 a
NR56	32.7 a	12.2 bc	5.9 d	13.2 c	36.0 c	64.0 a	2.28 a
NR79	30.7 a	15.3 a	7.5 c	13.1 c	33.4 c	66.6 a	2.31 a

Means with different letters in the same column are significantly different at the 0.05 level (LSD).

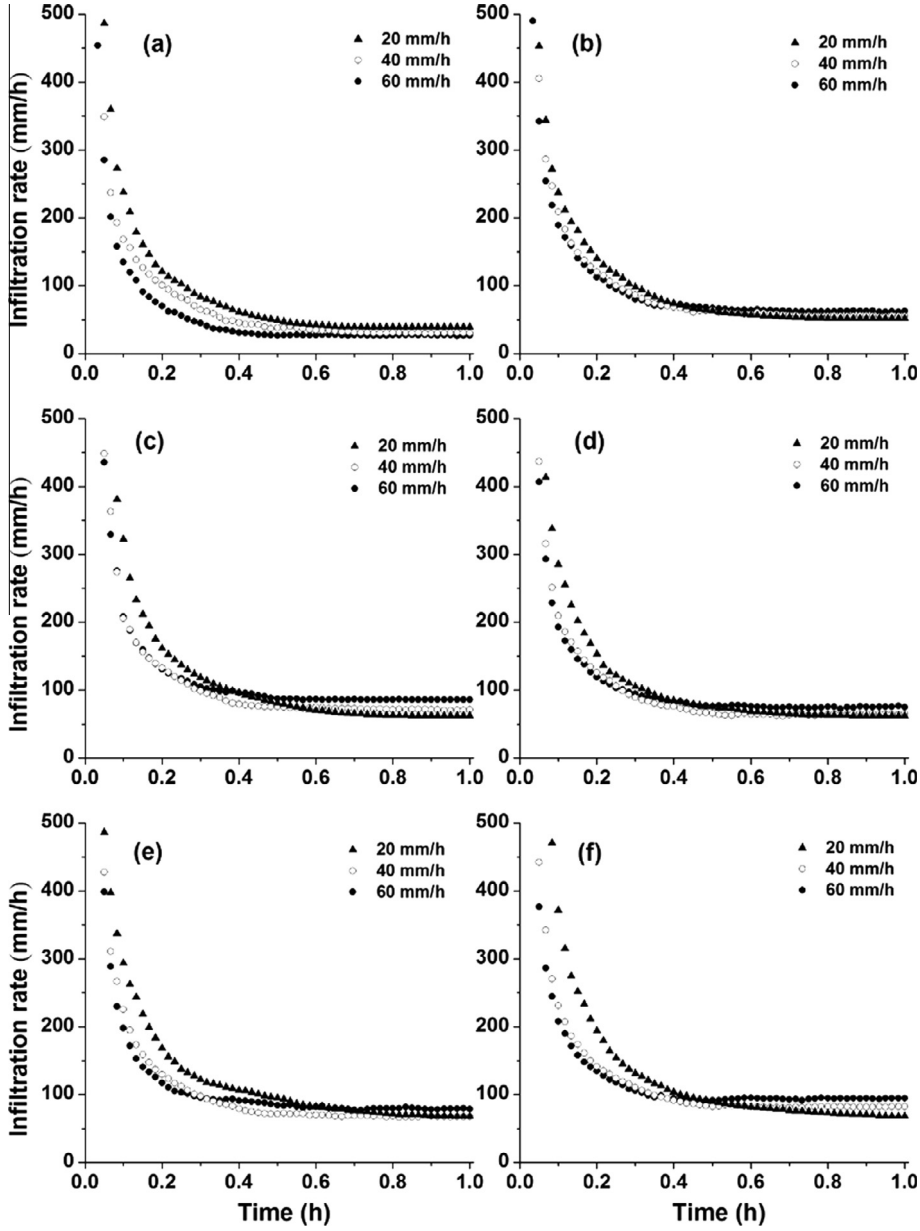

Fig. 4. Soil infiltration curves under different rainfall conditions (a) slope cropland, (b) natural vegetation restoration for 6-year, (c) 16-year, (d) 36-year, (e) 56-year, and (f) 79-year.

Table 4
Soil steady-state infiltration rate (SIR), time-to-runoff, time-to-SIR and runoff of slope cropland (SC) and abandoned 6- (NR6), 16- (NR16), 36- (NR36), 56- (NR56), and 79-year-old (NR79) naturally restored grasslands under different rainfall conditions.

Treatment	SIR (mm/h)			Time-to-runoff (min)			Time-to-SIR (min)			Runoff (L)		
	20 mm/h	40 mm/h	60 mm/h	20 mm/h	40 mm/h	60 mm/h	20 mm/h	40 mm/h	60 mm/h	20 mm/h	40 mm/h	60 mm/h
SC	39.3 a	30.2 b	27.0 c	38.8 a	19.9 b	6.4 c	57.3 a	42.7 b	25.0 c	0.04 c	4.04 b	10.45 a
NR6	52.2 b	55.4 b	62.4 a	ND	17.0 a	14.2 b	47.3 a	43.3 a	34.7 b	ND	1.85 b	5.52 a
NR16	62.5 c	71.5 b	86.4 a	ND	20.9 a	18.8 a	49.0 a	42.3 b	30.3 c	ND	0.61 b	2.81 a
NR36	62.6 b	64.9 b	75.1 a	ND	19.3 a	14.0 b	48.3 a	44.7 a	35.3 b	ND	2.05 b	3.53 a
NR56	67.7 b	67.9 b	81.0 a	ND	15.9 a	10.5 b	49.0 a	38.7 b	36.7 b	ND	1.02 b	3.91 a
NR79	68.5 c	82.1 b	95.4 a	ND	29.5 a	12.6 b	56.0 a	44.3 b	32.3 c	ND	0.27 b	2.53 a

Means with different letters in the same row under the same index are significantly different at the 0.05 level (LSD).
ND means not detected.

3.5. The relationship between water infiltration and soil properties

SOM content showed significantly positive linear relationships with macroaggregate (>0.25 mm) content as well as aggregate MWD (Fig. 7a). That is, the values of water-stable macroaggregate (>0.25 mm) content and aggregate MWD both increased with increasing SOM content. The SIR was significantly logarithmically correlated with SOM and macroaggregate (>0.25 mm) contents as

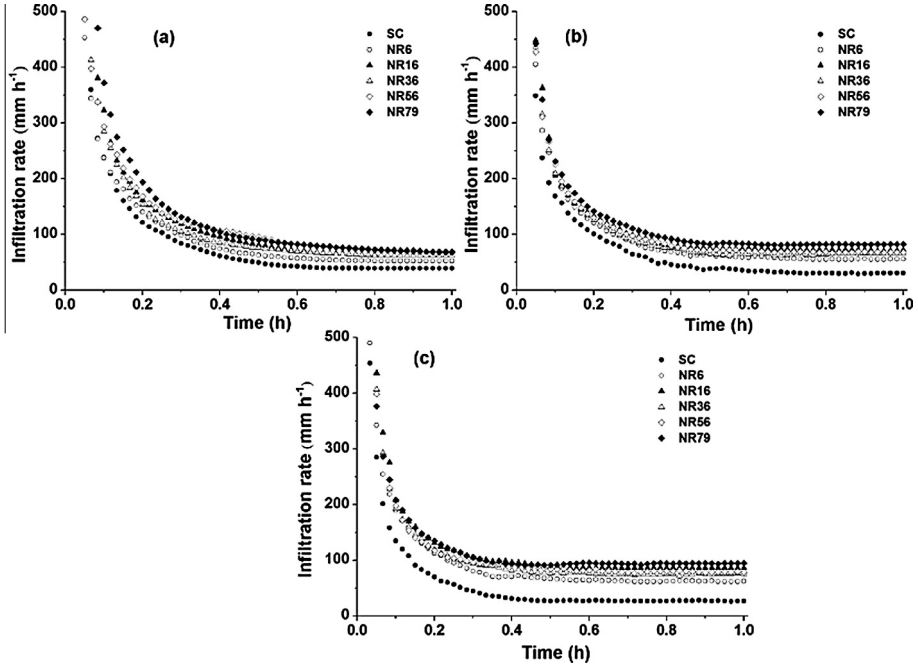

Fig. 5. Soil infiltration curves for natural restoration treatments at different rainfall intensities (a) 20 mm/h, (b) 40 mm/h, and (c) 60 mm/h.

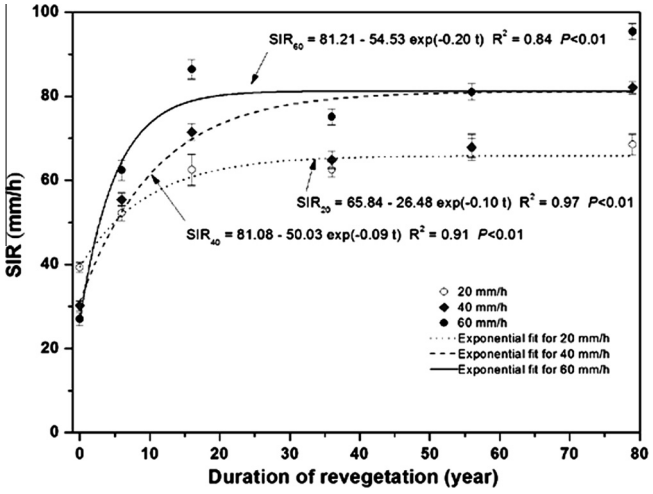

Fig. 6. Relationship between steady-state infiltration rate (SIR) and the period of natural vegetation restoration.

well as aggregate MWD under different rainfall conditions (Fig. 7b–d).

4. Discussion

4.1. Effect of soil properties on water infiltration

During the restoration of natural vegetation, soil properties are expected to undergo significant changes due to multi-factors. In the present study, we found that the SOM content and aggregate stability increased while the BD decreased with extending period of natural restoration (Table 2). These results are consistent with previous findings regarding the positive effects of vegetation restoration on soil physicochemical properties. A study found that natural vegetation restoration significantly decreased the BD and increased the porosity, aggregate stability, and saturated hydraulic conductivity of soil at the 0–20 cm depth in a 150-year chronological abandoned farmland on the Loess Plateau (Li and Shao, 2006). Jiao et al. (2011) reported that vegetation restoration had positive effects on SOM content and porosity and negative effect on the BD along a chronosequence of 5–45-year restored soils in northern Shaanxi, China. Similar results were found in a chronosequence of grassland in French Alps (Gros et al., 2004) and German Lahn-Dill Highlands (Breuer et al., 2006). The improvement of soil physicochemical properties with vegetation succession can be attributed to the accumulation of fresh plant residues in surface soil as well as roots and decomposed root residues in subsurface soil. These raw materials can be directly transformed into SOM and thus provide energy/carbon sources and nutrients for soil microorganisms (Golchin et al., 1994; Jastrow, 1996; Six et al., 2004, 1998), further promoting the development of soil aggregation (Six et al., 2000; Tisdall and Oades, 1982). Together these factors would induce the formation of macroaggregates and increase the water stability of aggregates (Angers and Caron, 1998; Gale et al., 2000; Kong et al., 2005). These explain the significant correlations between the SOM content and BD level as well as between the macroaggregate content and aggregate MWD (Fig. 7a), which are closely associated with soil infiltration (Fig. 7b–d).

Soil physicochemical properties and infiltrability were closely related to soil erosion in arid and semiarid regions. Under rainfall condition, soil erosion processes including material detachment and sediment transport mainly are strongly affected by raindrop impact and runoff flow (Lane et al., 1987). Greater soil losses are considered to be associated with less SOM content, poor aggregate stability, low IR, and high runoff rate (Lado et al., 2004a). In the present study, soil properties were found improved in terms of SOM content, structural property, and SIR during natural vegetation restoration, which might reduce the effects of rainfall and runoff flow on soil erosion. Moreover, the increase in infiltration and decrease in soil losses meant that larger volume of water could move into soil and less soil nutrition would be lost. These were of importance to promoting plant growth and maintaining soil quality in arid and semiarid environments.

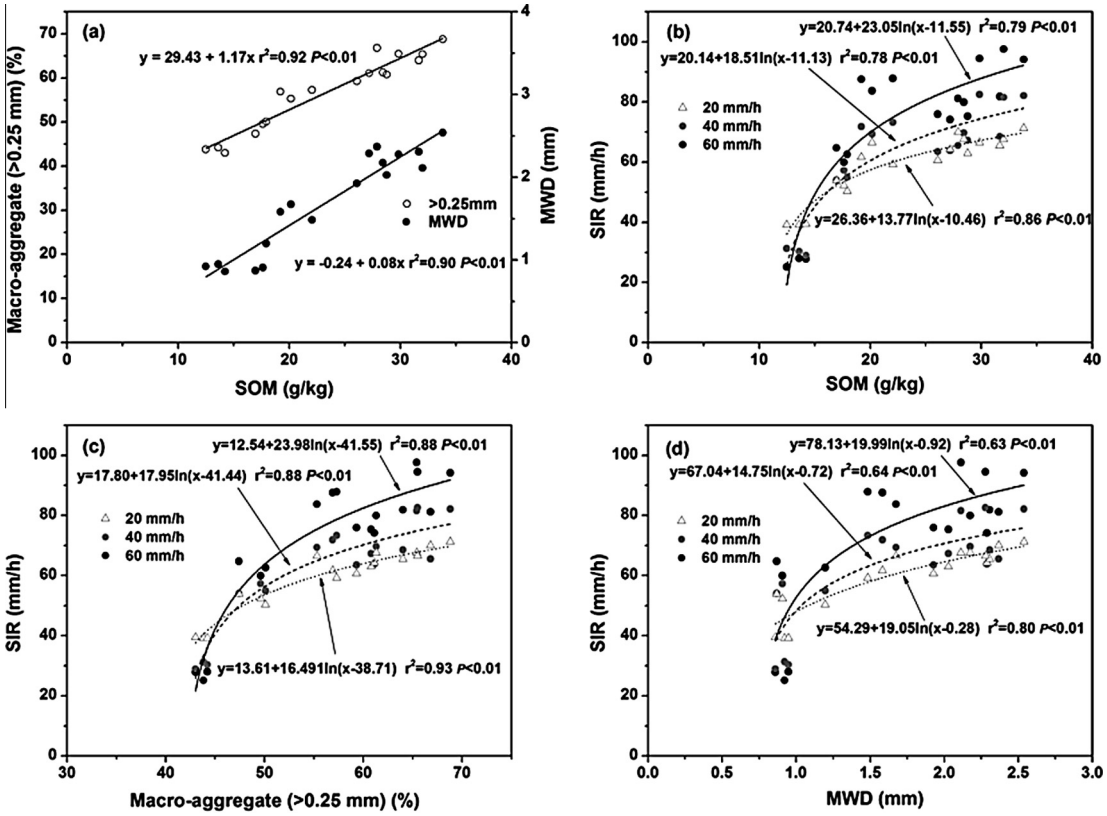

Fig. 7. Relationships between soil organic matter (SOM) content and (a) macroaggregate (>0.25 mm) proportion and mean weight diameter (MWD), and between steady-state infiltration rate (SIR) and (b) SOM, (c) macroaggregate (>0.25 mm), and (d) MWD.

4.2. Effect of rainfall intensity on water infiltration

For examination of infiltration, the run off–on–out method considers the influences of both rainfall and runoff that can affect seal formation in soil during rainstorm (Lei et al., 2006). With increasing intensity of rainfall, the IR obviously decreased in the control treatment (Fig. 4a). Likewise, the IR decreased in the natural restoration treatments within 30-min of simulated rainfall (Fig. 4b–f). These phenomena were consistent with previous laboratory observations by Lei et al. (2006) and Liu et al. (2011). The higher IRs under lower-intensity rainfall could be ascribed to the lower kinetic energy of rainstorm, which reduced the impact on aggregation in soil surface and thus increased infiltration (Shainberg et al., 1992; Smith et al., 1990). Compared with high-intensity rainfall, low-intensity rainfall with slow wetting rate could delay the declining rate of the hydraulic gradient and reduce the degree of aggregate slaking and breakdown (Lado et al., 2004b; Levy et al., 1997), thereby preventing seal formation and promoting water infiltration in soil (Lado et al., 2004b).

After 30-min simulated rainfall, the IRs of natural restoration treatments showed increasing trends as the intensity of rainfall was raised (Fig. 4b–f). This could be related to the differences in soil structural characteristics among the treatments during natural restoration. In general, soil structural properties determine the final infiltration capacity. Compared with the control treatment, the natural restoration treatments had higher porosity (lower BD) and more stable aggregation, that is, better ability of water infiltration. Despite the increasing intensity of rainfall, higher soil structural stability could reduce the susceptibility of water-droplet impact on soil surface (Abu-Hamdeh et al., 2006; Lado et al., 2004b; Zhang et al., 2007). None of the natural restoration treatments yielded positive data of runoff under low-intensity rainfall (20 mm/h). This observation indicated that compared to the slope cropland soil, the naturally restored grassland soil had improved infiltration capacity which enabled complete infiltration of the rainfall in both the run-on and run-off stages.

4.3. Effect of natural vegetation restoration period on water infiltration

Under different rainfall conditions, higher IRs were recorded in the older natural restoration treatments and a significant exponential relationship was found between the SIR and the period of natural vegetation restoration (Figs. 5 and 6). These results indicated that the process of natural vegetation restoration played a role in enhancing the infiltration of water into soil. Similar results were reported by Bo et al. (2007), who demonstrated with a disc infiltrometer that the SIR of abandoned cropland increased over time after 1-, 4-, and 8-year natural revegetation. A better soil infiltration capacity is commonly regarded as a fundamental change in soil structural properties such as higher aggregate stability and macroporosity of surface soil (Lipiec et al., 2006; Zhang et al., 2007). Franzluebbers (2002) demonstrated that greater surface SOM content and higher macroaggregate stability reduced the BD and improved water infiltration in soil. Many studies showed that better soil physical properties during natural vegetation restoration contribute to the improvement of soil hydraulic properties. In the present study, the SOM content and aggregate stability (indicated by MWD) gradually increased over time during natural grassland restoration (Tables 1 and 2). These results provide evidence that on the Loess Plateau, natural restoration of grassland effectively improved soil structural properties that are of importance to the infiltration process. This finding explains the changes in the infiltration capacity of soil across the chronosequence of natural grassland restoration.

Additionally, water IR is influenced by the distribution of roots in soil surface layer. The percentage root volumes at 0–10 cm soil depth of the 6-, 16-, 36-, 56-, and 79-year natural restoration treatments were 1.1%, 2.9%, 2.9%, 4.8%, and 5.7%, respectively. Correspondingly, the SIRs measured in the simulated rainfall experiment showed a rapidly increasing tendency from the control to 16-year natural restoration treatment, with relatively slow increases from the 36- to 79-year natural restoration treatments. Studies found that living roots increased the soil hydraulic conductivity by indirectly increasing soil macroporosity (Prieksat et al., 1994; Rachman et al., 2004). High macroporosity at the soil surface generally increased the IRs through the pattern of preferential flow (Beven and Germann, 1982; Ela et al., 1992; Hu et al., 2009). However, Gish and Jury (1982, 1983) found that living roots compacted soil and obstructed macropores, thereby reducing the hydraulic conductivity. In the present study, root distribution might have different effects on soil infiltration capacity. On one hand, the large IR recorded in the natural restoration treatments (<16-year) could be related to the large number of macropores associated with dead roots in soil. On the other hand, however, the larger amount of roots likely had restrictive influences on the soil infiltration capacity in the >16-year natural restoration treatments, as both the SOM content and aggregation stability showed pronounced improvement with increasing period of natural vegetation restoration. Because root characteristics could play an important role in soil infiltration during natural revegetation, detailed mechanisms through which the root characteristics affect infiltration need to be further studied.

Overall, 16-year after the conversion from cropland to natural grassland could be considered as a critical time point in the vegetation restoration process. Soil properties and infiltration were rapidly improved before this time point and underwent slight changes thereafter. These findings have implications for sustainable land use and soil management of the semiarid ecosystems. It is recommended to close abandoned cropland for approximately 16 years and then implement conservative grazing and suitable mow in order to regulate grassland growth and favor the development of farming and animal husbandry (Graetz and Tongway, 1986; Cheng et al., 1998).

5. Conclusions

On the Loess Plateau, the SIR decreased in slope cropland (control) and increased in naturally restored grasslands with increasing intensity of rainfall (20–60 mm/h). Under the same rainfall condition, the IR gradually increased with extending period of natural grassland restoration. During the process of natural restoration, higher infiltration capacity of soil was resulted from the elevation of SOM content and subsequent improvement of soil structural properties. Such changes might reduce the impact of rainfall on the formation of soil crust, accounting for the increased water IR and reduced runoff. Additionally, natural restoration of grassland for over 16-year showed generally stable soil structural properties and high infiltration capacity. These results are of guidance value for soil and water conservation on the Loess Plateau and potentially applicable to similar arid and semi-arid settings.

Acknowledgements

This work is jointly supported by the ‘Strategic Priority Research Program – Climate Change: Carbon Budget and Relevant Issues’ of the Chinese Academy of Sciences (Grant No. XDA05050504), the National High-tech R&D Program of China (863 Program) (Grant No. 2013AA102904) and the ‘111’Project (No. B12007).

References

Abu-Hamdeh, N.H., Abo-Qudais, S.A., Othman, A.M., 2006. Effect of soil aggregate size on infiltration and erosion characteristics. Eur. J. Soil Sci. 57 (5), 609–616.
Agassi, M., Shainberg, I., Morin, J., 1981. Effect of electrolyte concentration and soil sodicity on infiltration rate and crust formation. Soil Sci. Soc. Am. J. 45 (5), 848–851.
Agassi, M., Morin, J., Shainberg, I., 1985. Effect of raindrop impact energy and water salinity on infiltration rates of sodic soils. Soil Sci. Soc. Am. J. 49 (1), 186–190.
An, S.S., Huang, Y.M., Zheng, F.L., 2009. Evaluation of soil microbial indices along a revegetation chronosequence in grassland soils on the Loess Plateau, Northwest China. Appl. Soil Ecol. 41 (3), 286–292.
Angers, D.A., Caron, J., 1998. Plant-induced changes in soil structure: processes and feedbacks. Biogeochemistry 42 (1–2), 55–72.
Assouline, S., 2004. Rainfall-induced soil surface sealing: a critical review of observations, conceptual models, and solutions. Vadose Zone J. 3 (2), 570–591.
Ben-Hur, M., Lado, M., 2008. Effect of soil wetting conditions on seal formation, runoff, and soil loss in arid and semiarid soils—a review. Soil Res. 46 (3), 191–202.
Beven, K., Germann, P., 1982. Macropores and water flow in soils. Water Resour. Res. 18 (5), 1311–1325.
Blake, G.R., Hartge, K.H., 1986. Bulk density. In: Klute, A. (Ed.), Methods of Soil Analysis. Part 1: Physical and Mineralogical Methods. American Society of Agronomy, Madison, Wisconsin, USA, pp. 363–375.
Bo, H.F., Liu, G.B., Wang, G.L., 2007. Changes of infiltration characteristics of abandoned cropland with plant restoration in Loess Hilly region. Bull. Soil Water Conserv. 27 (3), 1–5 (31).
Breuer, L., Huisman, J.A., Keller, T., Frede, H.G., 2006. Impact of a conversion from cropland to grassland on C and N storage and related soil properties: analysis of a 60-year chronosequence. Geoderma 133 (1), 6–18.
Chartier, M.P., Rostagno, C.M., Pazos, G.E., 2011. Effects of soil degradation on infiltration rates in grazed semiarid rangelands of northeastern Patagonia, Argentina. J. Arid Environ. 75 (7), 656–661.
Cheng, J.M., Zou, H.Y., Akio, H., 1998. Effects of protective growing cutting and grazing on the vegetation of grassland. Res. Soil Water Conserv. 5 (1), 36–54.
Ela, S.D., Gupta, S.C., Rawls, W.J., 1992. Macropore and surface seal interactions affecting water infiltration into soil. Soil Sci. Soc. Am. J. 56 (3), 714–721.
Elliott, J.A., Efetha, A.A., 1999. Influence of tillage and cropping system on soil organic matter, structure and infiltration in a rolling landscape. Can. J. Soil Sci. 79 (3), 457–463.
Franzluebbers, A.J., 2002. Water infiltration and soil structure related to organic matter and its stratification with depth. Soil Tillage Res. 66 (2), 197–205.
Gale, W.J., Cambardella, C.A., Bailey, T.B., 2000. Root-derived carbon and the formation and stabilization of aggregates. Soil Sci. Soc. Am. J. 64 (1), 201–207.
Gish, T.J., Jury, W.A., 1982. Estimating solute travel times through a crop root zone. Soil Sci. 133 (2), 124–130.
Gish, T.J., Jury, W.A., 1983. Effect of plant roots and root channels on solute transport soils. Trans. ASAE 26 (2), 440–444.
Golchin, A., Oades, J.M., Skjemstad, J.O., Clarke, P., 1994. Soil structure and carbon cycling. Soil Res. 32 (5), 1043–1068.
Graetz, R.D., Tongway, D.J., 1986. Influence of grazing management on vegetation, soil structure and nutrient distribution and the infiltration of applied rainfall in a semi-arid chenopod shrubland. Aust. J. Ecol. 11 (4), 347–360.
Gros, R., Monrozier, L.J., Bartoli, F., Chotte, J.L., Faivre, P., 2004. Relationships between soil physico-chemical properties and microbial activity along a restoration chronosequence of alpine grasslands following ski run construction. Appl. Soil Ecol. 27 (1), 7–22.
Hu, W., Shao, M.A., Wang, Q.J., Fan, J., Horton, R., 2009. Temporal changes of soil hydraulic properties under different land uses. Geoderma 149 (3), 355–366.
Jastrow, J.D., 1996. Soil aggregate formation and the accrual of particulate and mineral-associated organic matter. Soil Biol. Biochem. 28 (4), 665–676.
Jiao, J.Y., Wang, W.Z., Hao, X.P., 1999. Precipitation and erosion characteristics of rain-storm in different pattern on Loess Plateau. J. Arid Land Resour. Environ. 13 (1), 34–42.
Jiao, J.Y., Tzanopoulos, J., Xofis, P., Bai, W.J., Ma, X.H., Mitchley, J., 2007. Can the study of natural vegetation succession assist in the control of soil erosion on abandoned croplands on the Loess Plateau, China? Restor. Ecol. 15 (3), 391–399.
Jiao, F., Wen, Z.M., An, S.S., 2011. Changes in soil properties across a chronosequence of vegetation restoration on the Loess Plateau of China. Catena 86 (2), 110–116.
Kong, A.Y., Six, J., Bryant, D.C., Denison, R.F., Van Kessel, C., 2005. The relationship between carbon input, aggregation, and soil organic carbon stabilization in sustainable cropping systems. Soil Sci. Soc. Am. J. 69 (4), 1078–1085.
Lado, M., Paz, A., Ben-Hur, M., 2004a. Organic matter and aggregate size interactions in infiltration, seal formation, and soil loss. Soil Sci. Soc. Am. J. 68 (3), 935–942.
Lado, M., Ben-Hur, M., Shainberg, I., 2004b. Soil wetting and texture effects on aggregate stability, seal formation, and erosion. Soil Sci. Soc. Am. J. 68 (6), 1992–1999.
Lane, L.J., Foster, G.R., Nicks, A.D., 1987. Use of Fundamental Erosion Mechanics in Erosion Prediction. Fiche No. 87-2540. American Society of Agricultural Engineers, St. Joseph, MI.
Lei, T.W., Liu, H., Pan, Y.H., Zhao, J., Zhao, S.W., Yang, Y.H., 2006. Run off–on–out method and models for soil infiltrability on hill-slope under rainfall conditions. Sci. China Ser. D 49 (2), 193–201.

Levy, G.J., Levin, J., Shainberg, I., 1997. Prewetting rate and aging effects on seal formation and interrill soil erosion. Soil Sci. 162 (2), 131–139.
Li, Y.Y., Shao, M.A., 2006. Change of soil physical properties under long-term natural vegetation restoration in the Loess Plateau of China. J. Arid Environ. 64 (1), 77–96.
Lipiec, J., Kuś, J., Słowińska-Jurkiewicz, A., Nosalewicz, A., 2006. Soil porosity and water infiltration as influenced by tillage methods. Soil Tillage Res. 89 (2), 210–220.
Liu, H., Lei, T.W., Zhao, J., Yuan, C.P., Fan, Y.T., Qu, L.Q., 2011. Effects of rainfall intensity and antecedent soil water content on soil infiltrability under rainfall conditions using the run off–on–out method. J. Hydrol. 396 (1–2), 24–32.
Nelson, D.W., Sommers, L.E., 1982. Total carbon, organic carbon, and organic matter. In: Page, A.L. (Ed.), Methods of Soil Analysis. Part 2: Chemical and Microbiological Properties. American Society of Agronomy, Madison, Wisconsin, USA, pp. 539–579.
Prieksat, M.A., Kaspar, T.C., Ankeny, M.D., 1994. Positional and temporal changes in ponded infiltration in a corn field. Soil Sci. Soc. Am. J. 58 (1), 181–184.
Rachman, A., Anderson, S.H., Gantzer, C.J., Thompson, A.L., 2004. Influence of stiff-stemmed grass hedge systems on infiltration. Soil Sci. Soc. Am. J. 68 (6), 2000–2006.
Shainberg, I., Levy, G.J., Rengasamy, P., Frenkel, H., 1992. Aggregate stability and seal formation as affected by drops' impact energy and soil amendments. Soil Sci. 154 (2), 113–119.
Shi, H., Shao, M.A., 2000. Soil and water loss from the Loess Plateau in China. J. Arid Environ. 45 (1), 9–20.
Six, J., Elliott, E.T., Paustian, K., Doran, J.W., 1998. Aggregation and soil organic matter accumulation in cultivated and native grassland soils. Soil Sci. Soc. Am. J. 62 (5), 1367–1377.
Six, J., Paustian, K., Elliott, E.T., Combrink, C., 2000. Soil structure and organic matter I. Distribution of aggregate-size classes and aggregate-associated carbon. Soil Sci. Soc. Am. J. 64 (2), 681–689.
Six, J., Bossuyt, H., Degryze, S., Denef, K., 2004. A history of research on the link between (micro) aggregates, soil biota, and soil organic matter dynamics. Soil Tillage Res. 79 (1), 7–31.
Smith, H.J.C., Levy, G.J., Shainberg, I., 1990. Water-droplet energy and soil amendments: effect on infiltration and erosion. Soil Sci. Soc. Am. J. 54 (4), 1084–1087.
Tang, K.L., Zhang, K.L., Lei, A.L., 1998. Critical slope gradient for compulsory abandonment of farmland on the hilly Loess Plateau. Chin. Sci. Bull. 43 (5), 409–412.
Tisdall, J.M., Oades, J.M., 1982. Organic matter and water-stable aggregates in soils. J. Soil Sci. 33 (2), 141–163.
van Bavel, C.H.M., 1950. Mean weight-diameter of soil aggregates as a statistical index of aggregation. Soil Sci. Soc. Am. J. 14, 20–23.
Wang, Y., Shao, M.A., Shao, H., 2010. A preliminary investigation of the dynamic characteristics of dried soil layers on the Loess Plateau of China. J. Hydrol. 381 (1), 9–17.
Yoder, R.E., 1936. A direct method of aggregate analysis of soils and a study of the physical nature of erosion losses. Agron. J. 28 (5), 337–351.
Zhang, G.S., Chan, K.Y., Oates, A., Heenan, D.P., Huang, G.B., 2007. Relationship between soil structure and runoff/soil loss after 24 years of conservation tillage. Soil Tillage Res. 92 (1–2), 122–128.
Zhu, X.M., 2006. Rebuild soil reservoir is an rational approach for soil and water conservation on the Loess Plateau. Bull. Chin. Acad. Sci. 21 (4), 320–324.
Zou, H.Y., Guan, X.Q., Zhang, X., Gu, X.L., 1997. Approach to management path way of Yunwushan Mountain Natural Protecting. Pratacult. Sci. 14 (1), 3–4.